

Researching Attitude-control Algorithm of Ejection Seats based on Time-sharing Strategy

Minghuan Zhang¹, Ming Wu², Yu Su¹ and Cheng Zhang¹

¹*School of Astronautics, Northwestern Polytechnical University, Xi'an, China*

²*Aerospace Life-Support Industries, LTD, Xiangyang, China*

Keywords: Ejection Seats, Attitude-control, Time-sharing Control, Minimum Safe Altitude, Optimization, Simulation.

Abstract: An attitude-control algorithm for ejection seats on “H” shaped motor is presented in this paper. The control algorithm is based on time-sharing strategy, and the parameters in algorithm are optimized by using PSO method. Through simulating under Matlab/Simulink in different ejection conditions, the infection of time-sharing strategy in attitude-control is analyzed, and the minimum safe altitude is compared with K36D-3.5A, ACES II and 120 ejection conditions in GJB 1800A-2007. The simulation results and analysis show that this control algorithm on “H” shaped motor can improve escape performance at low-altitude and adverse-attitude, thus proving the algorithm in this paper to be reliable and effective.

1 INTRODUCTION

Ejection seat is a key lifesaving appliance of modern fighter in emergency (Wang, 2014), and its core technology is attitude and trajectory control of the seat after ejection. Most of ejection seats in service at present are under the 3rd generation escape system. To improve the pilot's rescue, sequential control technology (used in the 3rd generation) is applied to make the seat for increasing the ejection altitude (Miles, 2015 and Wang, 2014). Along with high-tech of weapon, complexity of battlefield and quicken of combat rhythm, pilot would be highly possible to escape under low-altitude, adverse-attitude conditions or at extremely high speed.

Therefore, it is imperative to achieve adaptive control of ejection attitude. The 4th generation of ejection seat is designed to solve the rescue problem in low-altitude and adverse-attitude conditions beyond the current generation, and its core is the application of thrust vector continuous control technology (Ma,2000 and Keller, 2008). By the fast switching among thrust vector, the seat can gain maximal lift as quick as possible. Thereby, the safety is increased.

Technology on the 4th generation escape system was start to study from 1970s, however, it has not implemented for engineering application nowadays. One of the main technical bottlenecks is the application of thrust vector continuous control. U.S.

Air Force Research Lab proposed the structure of the ejection seat under the 4th generation escape system (Blairnald, 1998). The “H” shaped motor installed on the seat so that the nozzles located at four corners can obtain large moment arms for attitude-control. It makes maintaining a constant pressure become possible. (Feng, 2007) present a safe altitude impact factor method under the 3rd generation. It analyzed infection of aircraft parameters start from ejection to safe altitude. Despite this work can improved escape performance at medium-low-speed and lower-altitude somehow, it only meet 44% of the minimum safe altitude in GJB 1800-93. (Yuan, 2009) presents a nonlinear inverse-dynamics method to design the control law of the ejection seat under the 3rd generation. Results under medium-low speed can be verified in 4th generation escape system, but the robustness of this method need to be improved. Both of above two methods are based on sequential control technology. It can't meet the requirement of the adaptive control which is the symbol of the 4th generation.

We present a time-sharing attitude-control algorithm based on thrust vector continuous control technology. The parameters of controller is optimized by Particle Swarm Optimization(PSO). The experimental results and analysis show that this algorithm can achieve fast robust attitude-control of ejection seat. Moreover, this strategy gives a new

solution of adaptive control under 4th generation system.

2 MATHEMATICAL MODEL OF “H” SHAPED MOTOR

Fig.1 shows the “H” shaped motor installs at the ejection seat back. The motor is equipped with four fixed nozzle, which provide thrust for the ejection seat. Under body axis system, the thrust of each nozzle is shown as Eq.1 and Eq.2. $i = 1, 2, 3, 4$ refer to the nozzle number as the Fig.1 shows.

$$\begin{aligned} F_{hi_x} &= F_{hi} \sin \alpha_{hi} \cos \beta_{hi} \\ F_{hi_y} &= F_{hi} \cos \alpha_{hi} \\ F_{hi_z} &= (-1)^i F_{hi} \sin \alpha_{hi} \sin \beta_{hi} \\ i &= 1, 2 \end{aligned} \quad (1)$$

$$\begin{aligned} F_{hi_x} &= F_{hi} \sin \alpha_{hi} \cos \beta_{hi} \\ F_{hi_y} &= F_{hi} \cos \alpha_{hi} \\ F_{hi_z} &= (-1)^i F_{hi} \sin \alpha_{hi} \sin \beta_{hi} \\ i &= 3, 4 \end{aligned} \quad (2)$$

And the moment of each can be describe as Eq.3 and Eq.4.

$$\begin{aligned} M_{hi_x} &= (-1)^i F_{hi} \sin \alpha_{hi} \sin \beta_{hi} \cdot (L_{h1} - y_c) + \frac{(-1)^{i+1}}{2} F_{hi} \cos \alpha_{hi} \cdot L_{h2} \\ M_{hi_y} &= \frac{(-1)^i}{2} F_{hi} \sin \alpha_{hi} \cos \beta_{hi} \cdot L_{h2} + (-1)^i F_{hi} \sin \alpha_{hi} \sin \beta_{hi} \cdot x_c \end{aligned} \quad (3)$$

$$\begin{aligned} M_{hi_z} &= -F_{hi} \sin \alpha_{hi} \cos \beta_{hi} \cdot (L_{h1} - y_c) - F_{hi} \cos \alpha_{hi} \cdot x_c \\ i &= 1, 2 \end{aligned}$$

$$\begin{aligned} M_{hi_x} &= (-1)^{i+1} F_{hi} \sin \alpha_{hi} \sin \beta_{hi} \cdot y_c + \frac{(-1)^{i+1}}{2} F_{hi} \cos \alpha_{hi} \cdot L_{h2} \\ M_{hi_y} &= \frac{(-1)^i}{2} F_{hi} \sin \alpha_{hi} \cos \beta_{hi} \cdot L_{h2} + (-1)^i F_{hi} \sin \alpha_{hi} \sin \beta_{hi} \cdot x_c \end{aligned} \quad (4)$$

$$\begin{aligned} M_{hi_z} &= F_{hi} \sin \alpha_{hi} \cos \beta_{hi} \cdot y_c - F_{hi} \cos \alpha_{hi} \cdot x_c \\ i &= 3, 4 \end{aligned}$$

Nozzle #1 and nozzle #2 have the same installation angle direction, while nozzle #3 and nozzle #4 have the same installation angle direction. α_{hi} and β_{hi} are shown in the Fig.1 b) and c), in which i refers to the nozzle number.

When all four nozzles work at the same time, the total thrust and moment is shown as Eq.5 and Eq.6:

$$\begin{aligned} F_{hx} &= F_{h1_x} + F_{h2_x} + F_{h3_x} + F_{h4_x} \\ F_{hy} &= F_{h1_y} + F_{h2_y} + F_{h3_y} + F_{h4_y} \\ F_{hz} &= F_{h1_z} + F_{h2_z} + F_{h3_z} + F_{h4_z} \end{aligned} \quad (5)$$

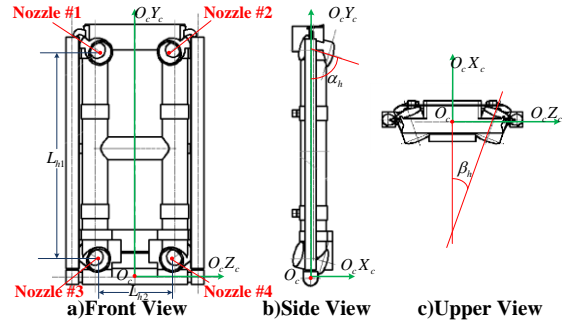


Figure 1: The structure of “H” shaped motor under body axis system.

$$\begin{aligned} M_{hx} &= M_{h1_x} + M_{h2_x} + M_{h3_x} + M_{h4_x} \\ M_{hy} &= M_{h1_y} + M_{h2_y} + M_{h3_y} + M_{h4_y} \\ M_{hz} &= M_{h1_z} + M_{h2_z} + M_{h3_z} + M_{h4_z} \end{aligned} \quad (6)$$

The motion attitude equations of ejection seat are:

$$\begin{aligned} \frac{d\vartheta}{dt} &= \omega_{y_t} \sin \gamma + \omega_{z_t} \cos \gamma \\ \frac{d\psi}{dt} &= (\omega_{y_t} \cos \gamma - \omega_{z_t} \sin \gamma) / \cos \vartheta \\ \frac{d\gamma}{dt} &= \omega_{x_t} - (\omega_{y_t} \cos \gamma - \omega_{z_t} \sin \gamma) \cdot \tan \vartheta \end{aligned} \quad (7)$$

In above, ϑ, ψ, γ refers to pitch, yaw and roll angle; $\omega_{x_t}, \omega_{y_t}, \omega_{z_t}$ are palstances around three axes under body axis system.

Attack and sideslip angle of ejection seat are α, β ;

$V_{x_t}, V_{y_t}, V_{z_t}$ is three velocity components of V_c :

$$\begin{aligned} V_c &= \sqrt{V_{x_t}^2 + V_{y_t}^2 + V_{z_t}^2} \\ \alpha &= \arctg(-V_{y_t} / V_{x_t}) \\ \beta &= \arcsin(V_{z_t} / V_c) \end{aligned} \quad (8)$$

3 ATTITUDE-CONTROL ALGORITHM

To maintain internal pressure balance, “H” shaped motor takes the control mode that each two nozzles has dual thrust vector. Once installation angle direction is set, it will not change through the all procedure. Thus, interconnection of each attitude angle between control moments is bad for the control algorithm design. We take the time-sharing control strategy. By optimizing installation angle direction of each nozzle, we can achieve decoupling of attitude-control moment.

3.1 Time-Sharing Control Algorithm

In time-sharing control strategy, “H” shaped motor

has three modes (pitch, yaw and roll mode). The thrust and moment of each is shown as Eq.9, Eq.10 and Eq.11.

Pitch mode:

$$F_{h1} = F_{h2} = \frac{K}{2} F_h, F_{h3} = F_{h4} = \frac{(1-K)}{2} F_h \quad (9)$$

$$M_x = M_y = 0$$

Yaw mode:

$$F_{h1} = F_{h3} = \frac{K}{2} F_h, F_{h2} = F_{h4} = \frac{(1-K)}{2} F_h \quad (10)$$

$$M_x = M_z = 0$$

Roll mode:

$$F_{h1} = F_{h4} = \frac{K}{2} F_h, F_{h2} = F_{h3} = \frac{(1-K)}{2} F_h \quad (11)$$

$$M_y = M_z = 0$$

F_h is the total thrust of the ‘‘H’’ shape motor, which is a constant value. K is the coefficient of each nozzle in dual control mode. The trust of four nozzle is determined totally by F_h and K .

We establish the inconsistent equations set on Eq.6 and three control modes. And optimize the installation angle of nozzles by finding optimal solution of this set. This is also the procedure of decoupling the control moment of three channels (Pitch, Yaw and Roll). Due to the specialization of inconsistent equations, coupling moments in three control mode can be zero at the same time. But the process of finding optimization ensures that residual coupling moment is far miner than the main control moment. Therefore, the residual coupling moment can be taken as small perturbation.

3.2 Algorithm Design

Under the time-sharing control strategy, the time of each channel is limited. The attitude-control is further weakened by constraint of ejection altitude. If control time is mainly spent on decoupling of palstances, attitude-control period could be delayed. If ignore the decoupling and concentrate on attitude-control, the speed of attitude-control will be slow, and even influence the stability of the system. Finally, trajectory control will be affected.

To minimize the motion decoupling, we take a switching strategy between coupling palstances and attitude to achieve fast control of attitude.

3.2.1 Control Objective

Set $(\vartheta, \beta, \gamma, \dot{\vartheta}, \dot{\psi}, \dot{\gamma})$ (refers to pitch, yaw, roll, pitch palstance, yaw palstance and roll palstance) as control variables, and its expectation is signed as

$(\vartheta^*, \beta^*, \gamma^*, \dot{\vartheta}^*, \dot{\psi}^*, \dot{\gamma}^*)$. To maintain the stability of system, $\dot{\vartheta} = \dot{\psi} = \dot{\gamma} = 0^\circ / s$; To ensure that the seat can get the maximum lift, the expectation of roll is $\gamma^* = 0^\circ$ and yaw is $\beta = 0^\circ$ by adjustment of ψ^* . According to finding the optimization of inconsistent equations, installation angle direction of nozzle after decoupling is $\alpha_{h1} = 40^\circ, \alpha_{h2} = 58^\circ, \beta_{h1} = 72.5^\circ, \beta_{h2} = 7^\circ$. When the pitch expectation is $\vartheta^* = 38^\circ$, the lift can be maximum, and expectation of control variable is :

$$(\vartheta^*, \beta^*, \gamma^*, \dot{\vartheta}^*, \dot{\psi}^*, \dot{\gamma}^*) = (38^\circ, 0^\circ, 0^\circ, 0^\circ / s, 0^\circ / s, 0^\circ / s)$$

3.2.2 Transfer Function

To design the control system, the transfer function between K and control variable:

$$\frac{\dot{\vartheta}(s)}{K(s)} = -\frac{a_3s + a_3a_4}{s^2 + a_4s + a_2}$$

$$\frac{\beta(s)}{K(s)} = -\frac{b_3}{s^2 + b_4s + b_2}$$

$$\frac{\dot{\psi}(s)}{K(s)} = -\frac{b_3s + b_3b_4}{s^2 + b_4s + b_2}$$

$$\frac{\dot{\gamma}(s)}{K(s)} = -\frac{c_3}{s} \quad (12)$$

In above, a_2, b_2 is static stability of related control channel. a_3, b_3, c_3 is the efficiency coefficient, which refers to palstance increment of related control channel when K increase. a_4, b_4 is the palstance increment of trajectory tangent line.

3.2.3 Linear Systems Control Design

Take pitch control channel as example, the system block diagram is shown as Fig.2. e_ϑ is the difference of pitch expectation and actual value; K_p, K_I, K_D refers to gain of proportion, integration and differentiation in PID algorithm; K (thrust partition coefficient of nozzles in pitch channel) can be calculated by K_p, K_I, K_D and current e_ϑ .

In order to maintain the dynamic performance of this control system, K_p, K_I, K_D can be optimized through PSO method.

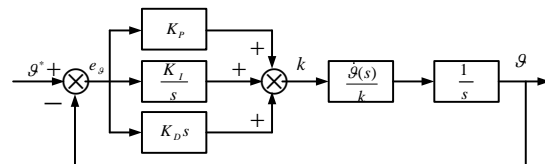


Figure 2: Control block diagram of pitch channel.

Velocity and position of particle in search space can be described as:

$$\begin{aligned} v_{i+1} &= wv_i + c_1r_1(P_i - a_i) + c_2r_2(G_i - a_i) \\ a_{i+1} &= a_i + v_{i+1} \end{aligned} \quad (13)$$

In which, a is the particle position and v is velocity. w is inertia factor and c_1, c_2 are acceleration constants. r_1, r_2 are random values between $[0,1]$. $P_i = [K_p, K_I, K_D]$ is the optimal control parameter of particle so far and $G_i = [\overline{K_p}, \overline{K_I}, \overline{K_D}]$ is the whole Particle Swarm's best parameter so far.

The optimization flow chat of PSO algorithm in pitch channel shows as follows:

- Step 1 Initialize all the particle's position and velocity in swarm, and set optimum control parameters P_i and G_i ;
- Step 2 Check whether the adaptive factor of every particle is better than optimum control parameter P_i , if yes, update the P_i to current particle adaptive factor;
- Step 3 Check whether the adaptive factor of every particle is better than optimum control parameter G_i , if yes, update the G_i to current particle adaptive factor;
- Step 4 Update particle's position and velocity use Eq.13;
- Step 5 If the iterative step meet the max value or the particle adaptive factor smaller than lower limit, exit and get optimum value. Otherwise, return to Step 2.

The parameters in PSO algorithm are as follows:

- Inertia factor is $w = 0.6$;
- Acceleration constants are $c_1 = c_2 = 2$;
- Iteration number is 100;
- Particle number is 100;
- Minimum particle adaptive factor is 0.1.

K of each channel can be obtained:

$$K = \begin{cases} K_{p1}e_\theta + K_{I1} \int e_\theta dt + K_{D1} \frac{de_\theta}{dt} & \text{pitch} \\ K_{p2}e_\beta + K_{I2} \int e_\beta dt + K_{D2} \frac{de_\beta}{dt} & \text{yaw} \\ K_{p3}e_\gamma + K_{I3} \int e_\gamma dt + K_{D3} \frac{de_\gamma}{dt} & \text{roll} \\ K_{p4}\dot{\theta} + K_{I4} \int \dot{\theta} dt + K_{D4} \frac{d\dot{\theta}}{dt} & \text{pitch palstance} \\ K_{p5}\dot{\psi} + K_{I5} \int \dot{\psi} dt + K_{D5} \frac{d\dot{\psi}}{dt} & \text{yaw palstance} \\ K_{p6}\dot{\gamma} + K_{I6} \int \dot{\gamma} dt + K_{D6} \frac{d\dot{\gamma}}{dt} & \text{roll palstance} \end{cases} \quad (14)$$

According to PSO results, gains of each control channel are shown as Eq.15 and Fig.3.

$$\begin{aligned} K_{p1} &= 6, K_{p2} = K_{p3} = K_{p4} = K_{p5} = K_{p6} = 3 \\ K_{I1} &= \begin{cases} -0.5 & -180^\circ \leq \alpha < -70^\circ \\ 0.9 & -70^\circ \leq \alpha < 10^\circ \\ -0.8 & 10^\circ \leq \alpha < 80^\circ \\ 0.5 & 80^\circ \leq \alpha < 180^\circ \end{cases} \\ K_{I2} = K_{I3} &= 0, K_{I4} = K_{I5} = K_{I6} = 10 \\ K_{D1} &= 0.8, K_{D2} = K_{D3} = 0.5, K_{D4} = K_{D5} = K_{D6} = 0 \end{aligned} \quad (15)$$

3.2.4 Switching Control Strategy

Our switching control strategy of coupling palstances and attitude is illustrated as Fig.4.

4 SIMULATION RESULTS AND ITS ANALYSIS

Based on 120 ejection conditions which is regulated by GJB 1800-2007 (General Specification for Ejection Seat Type of Aircrew Emergency Escape System), we experiment under Matlab/Simulink simulation environment. And we verify the performance of attitude-control algorithm by minimum safe altitude and changing curve of attitude angle after ejection.

We display simulation results under four type conditions. The simulation time is 1.8s and the simulation step is 0.001s. Fig.5 shows the changing curves of attitude angle after ejection.

It is noted that all the angle and velocity here refers to the angle and velocity of aircraft under inertial frame. As simulation results, curves in red is pitch, curves in blue is roll and curves in green is roll.

Fig.5 a) and b) shows the simulation results of large roll angle attitude.

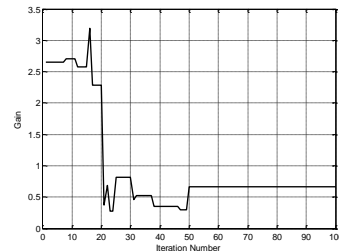


Figure 3: The optimization curve of PSO.

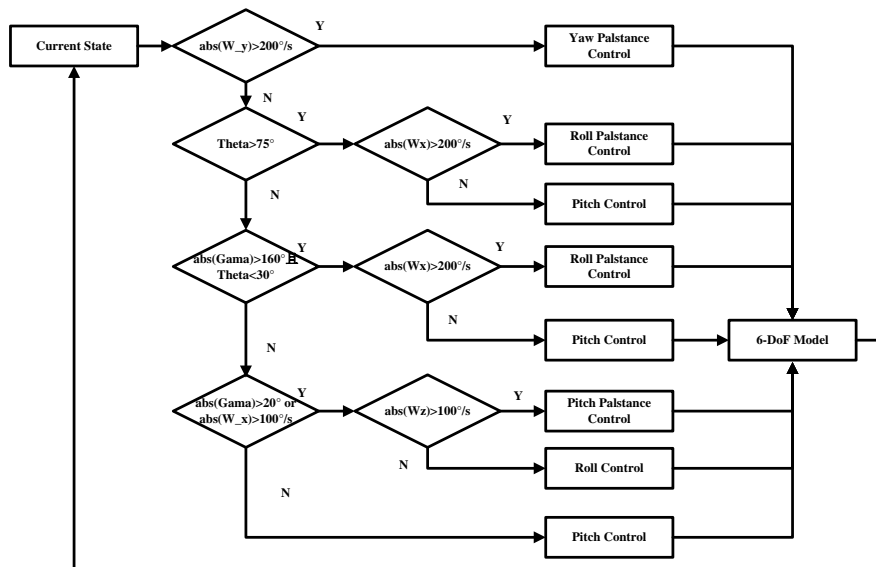


Figure 4: Switching control strategy.

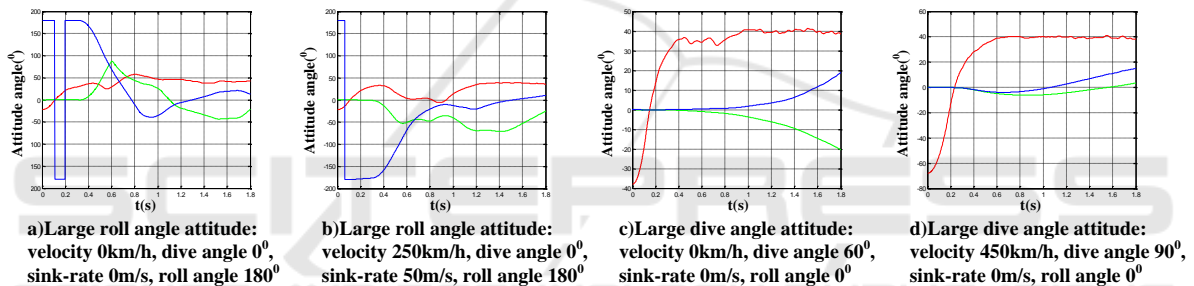


Figure 5: Curves of attitude angle in adverse conditions.

Due to the time-sharing strategy, the system is in pitch control channel from 0-0.35s in Fig.5 a). Since the initial aerodynamic-force is too low to take into consideration, the roll angle has not changed in this period; The roll angle is close to the control target 38° around 0.35s, so we switch the system to roll control channel. During the period of 0.35-1.2s the system is under roll control channel, pitch angle has drifted in some extend due to the increase of aerodynamic-force and infection of coupling palstances. The system enters stability augumentation control condition after 1.2s; Roll and pitch angle are around the control target during 1.2-1.8s. In the whole process, the velocity of ejection seat is quite small, therefore the infection of aerodynamic moment from sideslip-angle is not big and the control period is quite short.

Similarly in Fig.5 b), during the time period 0-0.4s and 0.4-1s, roll angle control and pitch angle control has been affected due to the switching

strategy. In addition, the pitch and roll channel realize fast attitude stable.

Fig.5 c) and d) shows the simulation results of large dive angle attitude. The system can achieve fast stable of pitch attitude within 0.5s. Because “H” shaped motor has symmetric control moment in pitch channel and coupling moment of roll and yaw is negligible, the change of roll and sideslip-angle is too small to affect dynamic performance of the system.

From simulation results, this time-sharing strategy can achieve fast, effective and stable control of ejection seat attitude.

We compare our results with the minimum safe altitude requirement of ACES II, K36D-3.5A in adverse conditions (Barnette, 1998) in Tab.1. The minimum safe altitude is $h = \min(0, h_1 - h_2)$, h_1 is the altitude when ejection and h_2 is the lowest altitude of movement curve.

Table 1: Comparison of minimum safe altitude.

No.	Aircraft Attitude		Velocity (KEAS)	Minimum Safe Altitude(ft)		
	Dive Angle(°)	Roll Angle(°)		ACES II	K36D-3.5A	Our Results
1	0	60	120	0	0	0
2	0	180	150	150	96	91
3	0 ¹	0	150	116	137	66
4	60	0	200	335	288	259
5	30	0	450	497	518	454
6	60	60	200	361	299	331
7	45	180	250	467	323	353

Notes: 1. The current sink-rate of aircraft is 10,000ft/min;
 2. KEAS (Knots Equivalent Air Speed) is 1knot=1.85km/h.

In the first 5 states in Tab.1, our minimum safe altitudes are all lower than that in ACES II and K36D-3.5A; And the following two are better than ACES II.

GJB 1800-2007 regulates 120 conditions, 88 of which is low speed and 32 is high speed. By experimental comparison, our algorithm can meet the 67 conditions in low speed, about 76%. In high speed, 24 conditions can meet the requirement, about 75%. Based on ejection seat with “H” shape motor, our algorithm can effectively increase the ejection altitude and therefore improve the occupant’s rescue.

5 CONCLUSIONS

This paper proposes an attitude-control algorithm for ejection seats based on time-sharing control strategy. The parameters of controller are optimized by applying PSO method. Simulation results show that our algorithm can meet the requirement of 75% conditions in GJB 1800-2007, which included low-altitude, adverse-attitude and some of the high speed conditions. Based on continuous thrust vector control framework, our approach is designed totally under 4th generation escape system. Experiment and its analysis verify that our approach can feasibly and effectively achieve adaptive control.

ACKNOWLEDGEMENTS

This work is supported by the National Natural Science Foundation of China (No.61502391), the China Space Foundation (No.N2015KC0121).

REFERENCES

- Wang, Y., F., Han, L., L., Wang, F., 2014. Review of Ejection Seat Electronic Program Controller. *Applied Mechanics and Materials*, 551: 530-534.
- Miles, J, E., 2015. Factors Associated with Delayed Ejection in Mishaps Between 1993 and 2013. *Aerospace Medicine and Human Performance*, 86(8): 774-781.
- Wang, Y., F., Chen, G., Han, L., L., 2014. The Comprehensive Survey for the Numerical Simulation of the 4th Generation Rocket Ejection Seat Thrust Vector Control System. *Design, Manufacturing and Mechatronics*, 551: 523-529.
- Ma, D., Obergefell, L., Rizer, A., et al, 2000. Biodynamic Modeling and Simulation of the Ejection Seat/Occupant System. *Biodynamic Modeling & Simulation of the Ejection Seat/occupant System*.
- Keller, K., Plaga, J., 2008. The Ejection Seat Test Database: A Resource for Enabling Aircrew Safety and Survivability. *AIR FORCE RESEARCH LAB WRIGHT-PATTERSON AFB OH BIOMECHANICS BRANCH*.
- Blairnald, A., 1998. 4TH Generation Escape System Technologies Demonstration Phase II. *Generation Escape System Technologies Demonstration Phase II*.
- Feng, W., C., Lin, G., P., 2007. Multi-parameter and Multi-mode Control Simulation Analyses of Ejection Seat. *Journal of System Simulation*, 19(10): 2283-2286.
- Yuan, W., M., 2009. Research on Attitude-Control Project of the Ejection Seats. *Nanjing: Nanjing University of Aeronautics and Astronautics*.
- Barnette, B., Peterson, K., L., 1998. MAXPAC Update and Lessons Learned. *Proceeding of the 36th Annual SAFE Symposium, America: SAFE Association*.